# Wheel Torque Optimization for a Compliant Modular Robot


Avinash Siravuru
Robotics Research Centre
IIIT-Hyderabad
Hyderabad, India
avinash.siravuru@research.iiit.ac.in

Suril V Shah
Robotics Research Centre
IIIT-Hyderabad
Hyderabad, India
surilshah@iiit.ac.in

K Madhava Krishna
Robotics Research Centre
IIIT-Hyderabad
Hyderabad, India
mkrishna@iiit.ac.in



***Abstract*—This paper proposes a systematic method to optimize wheel torques in a compliant modular robot, which consists of 3 link-wheel modules connected by revolute joints. Conventionally, actuators are used at these joints for posture control while climbing. In this work, use of torsional springs at the joints is proposed for posture control. The compliance thus obtained is profitably used to manoeuvre on uneven terrains. It is also shown how the springs are designed to be stiff enough to restrict the link-wheel module from tipping over while climbing big step-like obstacles. The only actively controlled variables of the robot are wheel torques, which are optimized to minimize wheel slip. This helps in reducing odometric error and maximizing energy efficiency. The proposed optimization builds on the quasi-static analysis of the robot and forms one of the key novelties of this paper. The results show the advantages of modularity in climbing big steps without any slip. The proposed wheel-torque optimization lends utility in the design of an appropriate wheel velocity controller.**


## I. Introduction

The aim of this paper is to present a method to perform wheel torque optimization on a compliant modular robot, used for climbing big steps and other forms of structured obstacles found in human populated environments. In the past, research on robots for uneven terrain traversal led to the development of two classes of vehicles. They are, 1) Passive Suspension Mechanisms and 2) Active Suspension Mechanisms. Passive suspension mechanisms, like Rocky7 [12] and Shrimp [2] use only wheel actuators for motion and manage to climb obstacles up to twice their wheel diameter. The fact that they do not employ any additional actuation for posture control, comes at the cost of a complex design. On the other hand, active suspension systems like Hylos [3] and PAW [11] have simpler designs but they need additional actuation to control their posture. So far, modular robots have been a key sub-class of active suspension robots, and they have been widely used in urban search and rescue operations [13].

Modular Robots offer many advantages. Firstly, the motor power is distributed. Therefore, several low torque motors can be used to realize the desired posture. This also helps in reducing the size of each individual module. Secondly, the redundancy helps in freely deforming along different types of obstacles. Especially, in urban search and rescue missions (for example, during earthquakes), it is necessary to have robots which can navigate through cluttered spaces (through pipes, rubble, etc.) or on highly unstructured terrains. Thirdly, as it is modular, it can still function with limited capability in spite of some modules malfunctioning, as opposed to its single module counterparts. Though modular robots can be controlled to follow desired trajectories with stable postures (such that the robot doesn't tip over), a lot of actuators need to be used in this process.

It is desirable to have a simple modular mechanism requiring no additional actuation to control its posture while navigating on an uneven terrain. Literature on passive modular robots is less common as it is very challenging to control the internal mobility of highly redundant robots while climbing, without any additional link actuation. The aim of this paper is to propose a novel modular robot which can successfully climb step-like obstacles with minimal slip and without any link actuation. Springs are used at the link joints to passively allow stable postures and restrict unstable postures by stiffening when required. The stiffness of the springs is determined to achieve this effect.

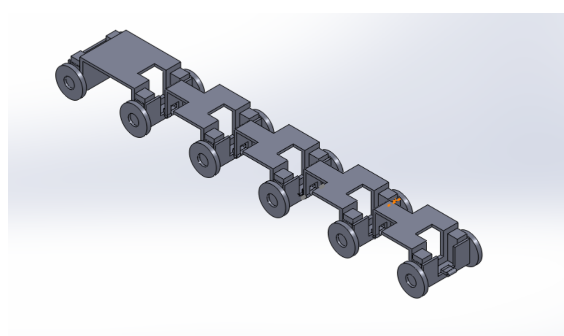

Fig. 1: CAD model of the proposed 3-module robot

Figure 1 shows the isometric and the front views of the robot mechanism. Note that, the analysis in this paper is

Proceedings of the 1st International and 16th National Conference on Machines and Mechanisms (iNaCoMM2013), IIT Roorkee, India, Dec 18-20 2013

limited to 3 link-wheel modules. This modular robot relies on wheel actuation for its terrain traversal, and it is the only parameter that can be controlled to maintain static equilibrium. However, this is valid only when the wheels are rolling without slipping. So it is very crucial to ensure that slippage is kept low so that the robot can be better controlled. This is a key motivation for proposing the wheel torque optimization, which will be explained in the subsequent sections of this paper.

The remaining paper is organized as follows. In Section II, the modular robot mechanism is introduced, and its quasi-static analysis is provided. The estimation of stiffness for the springs used in passive posture control is also described. Section III introduces wheel slip and presents a systematic procedure to perform wheel torque optimization with an objective to minimize slippage. Section VI discusses the results obtained from the optimization routine while Section V contains the conclusions and outline for future work.

## II. Model Description

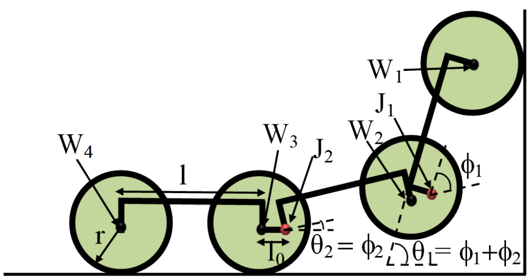


Fig. 2: Schematic of the 3-module robot

Figure 2 shows a snapshot of the proposed robot mechanism consisting of 3 links and 4 wheel-pairs. Each link and wheel pair form a module. The link-joints are positioned at the same height as that of the wheel axes with suitable offset. The joints at wheels and links are denoted by $W_1 - W_4$ and $J_1 - J_2$, respectively. The aim of this paper is to only use the traction forces developed at the wheel-ground contacts to climb steps. The passive link joints allow the mechanism to freely deform along an obstacle. When the first wheel comes in contact with the step, a normal force is developed in the horizontal direction. This equals the sum of traction forces of the remaining wheels. This can be proved using the static equilibrium equations(along the x-direction) of the mechanism for that instant, as shown in (2). The moment generated by this normal force lifts the first wheel off the ground and along the step. Thus the robot begins to climb steps by the virtue of only the traction forces of its wheels. Sufficient clearance, $c$, is provided to ensure that the links do not collide with the obstacles during their climbing motion. A more comprehensive discussion on the robot's design is given in [1]. The Specifications of the robot are provided in Table I.

TABLE I: Specifications of the Robot

| Symbols | Quantity | Values(with Units) |
|---|---|---|
| $l$ | Link Length | 0.15 $m$ |
| $b$ | Link Breadth | 0.1 $m$ |
| $r$ | Wheel Radius | 0.03 $m$ |
| $l_0$ | Wheel Joint and Link Joint Offset | 0.03 $m$ |
| $\tau_{wmax}$ | Stall Torque of Wheel Motors | 0.6 $Nm$ |
| $m_w$ | Mass of Each Wheel | 0.1 $Kg$ |
| $m_l$ | Mass of Each Link | 0.3 $Kg$ |

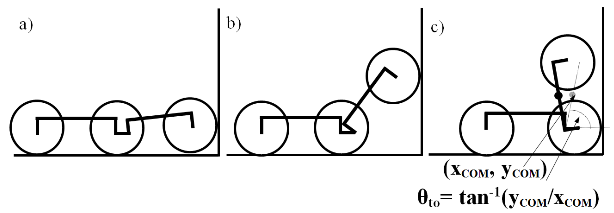


Fig. 3: A fully passive system failing to climb a big step like obstacle

### A. Stability Analysis of the Passive Mechanism

Stability analysis for a passive mechanism helps in determining postures of the robot for climbing steps without tipping over. In this subsection, some design parameters are first defined, and will be used in subsequent sections for the purpose of analyses. Let $\phi_i$ be the relative joint angle between links $i$ and $i+1$ and $\theta_i$ be the absolute joint angle of link $i$ with respect to the ground, as shown in Fig. 2. When only one link is climbing at any instant, $\theta_1 = \phi_1$. While climbing steps smaller than its link length, the maximum angular displacement occurs at the top most point of the step. Hence, it can be seen that as the step height increases, $\theta_1$ also increases till a certain $\theta_{1max}$. For the proposed robot design, $\theta_{1max} = \phi_{1max} = 72^0$. For step heights nearly equal to the link length, $\theta_{1max}$ approaches $72^0$. Beyond this point, the moment due to the normal force and self weight will both act in the counter clockwise direction causing the link to tip-over. Thus the system fails to climb heights nearly equal to or greater than it's link length. Figs. 3(a)-3(c) illustrate how a 2-linked passive modular robot with a similar mechanism fails to climb a step of height greater than its link length. This is a major drawback of the fully passive system. The angle at which the link begins to tip-over is called the tip-over angle and denoted by $\theta_{to}$, as shown in the Figure 3(c). This can be calculated using the position of the link-wheel module's center-of-mass(COM) as $\theta_{to} = pi/2 - tan^-1(y_{COM}/x_{COM})$, where $(x_{COM}, y_{COM})$ denote the x and y coordinates of the COM, respectively. It can be clearly seen that, for a uniform mass distribution, as the ground clearance of the robot increases, the value of $\theta_{to}$ decreases. For the proposed robot, $\theta_{to}$ is $72^0$.

Alternative methods need to be explored to restrict the links from going past the tip-over angle $\theta_{to}$ and subsequently climb bigger steps without tipping over. Ideally, this should be achieved without any major modification to the existing mechanism. While the many degrees-of-freedom (DOF) of the robot help in climbing obstacles by freely deforming along their contours, they also make it susceptible to tip over while climbing steep obstacles. Taking this into consideration, the mechanism should be smartly modified to freely allow deformation against smaller angular displacements and constrain it when the angular displacements are larger leading to failure. Spring compliance could be a potential choice provided the stiffness is carefully determined. The advantages of springs are detailed in [9] and this paper is inspired from that work. To determine the optimal stiffness, it is important to first determine the moments generated at the respective link joints when the relative angles($\phi$'s) between the links approach tip-over angles($\theta_{to}$). To obtain the same, a quasi-static model of the robot is developed and the static stability equations are derived to determine spring stiffness.

### B. Quasi-Static Model of the Modular Robot

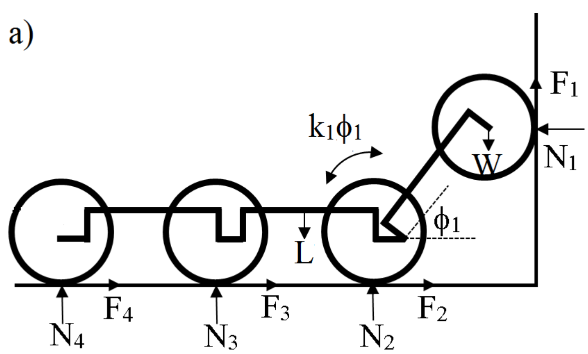


(a) Phase-1: one link climbing at any instant

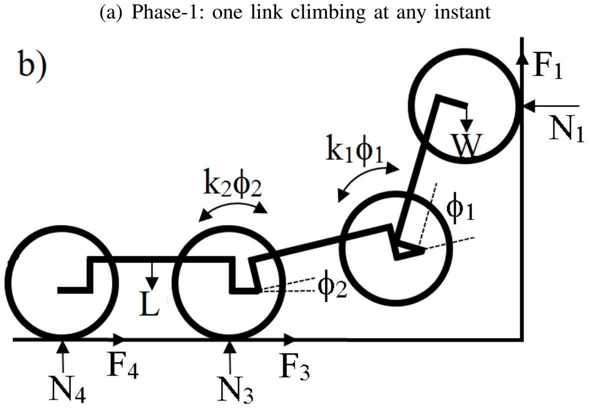


(b) Phase-2: two links climbing at any instant

Fig. 4: Snapshots showing the various forces and moments acting on the robot during the 2 climbing phases

The quasi static analysis of the robot is performed in two phases. This division is essential as the forces and moments acting on the robot change from one phase to the other. Every time a wheel-pair lifts off the ground, its corresponding normal and traction force are lost and an additional counter moment is generated due to the spring at the respective link joint. This changes the $\sum F_y$ (net force acting in the y -direction), $\sum F_x$(net force acting in the x-direction) and $\sum M$'s (net moments about $J_1$ and $J_2$), which have to be appropriately adjusted to maintain static equilibrium. Therefore, when every subsequent wheel is lifted off the ground, the robot transits from one climbing phase to the other. This analysis assumes the robot to be planar as the robot is symmetric along the sagittal plane.

$$
\begin{aligned}
&\sum F_x = 0 && N_1 - F_2 - F_3 - F_4 = 0 \\
&\sum F_y = 0 && 3w_l + 4w_w - F_1 - N_2 - N_3 - N_4 = 0 \\
&\sum M_{J_1} = 0 && F_1(lcos\theta_1 + r - csin\theta_1) + N_1 lsin\theta_1 \\
& && - w_l[(l/2)cos\theta_1 - csin\theta_1] - k_1\phi_1 \\
& && - w_w(lcos\theta_1 - csin\theta_1) = 0 \\
&\sum M_{J_2} = 0 && F_2 r + N_2 l - w_w l - w_l(l/2) \\
& && - [2(w_w + w_l) - F_1]l - k_1\phi_1 + k_2\phi_2 = 0 \\
&\sum M_{R3} = 0 && F_3 r + N_3 l - w_w l - w_l(l/2) \\
& && - [3(w_w + w_l) - F_1 - N_2]l + k_2\phi_2 = 0
\end{aligned}
\tag{1}
$$

$$
\begin{aligned}
&\sum F_x = 0 && N_1 - F_3 - F_4 = 0 \\
&\sum F_y = 0 && 3w_l + 4w_w - F_1 - N_3 - N_4 = 0 \\
&\sum M_{J_1} = 0 && F_1(lcos\theta_1 + r - csin\theta_1) + N_1 lsin\theta_1 \\
& && - w_l[(l/2)cos\theta_1 - csin\theta_1] - k_1\phi_1 \\
& && - w_w(lcos\theta_1 - csin\theta_1) = 0 \\
&\sum M_{J_2} = 0 && - [2(w_l + w_w - F_1)(lcos\theta_2 - csin\theta_2)] \\
& && - w_l[(l/2)cos\theta_2 - csin\theta_2] + k_1\phi_1 - k_2\phi_2 \\
& && - w_w(lcos\theta_2 - csin\theta_2) + N_1 lsin\theta_2 = 0 \\
&\sum M_{R3} = 0 && F_3 r + N_3 l - w_w l - w_l(l/2) \\
& && - [3(w_w + w_l) - F_1]l + k_2\phi_2 = 0
\end{aligned}
\tag{2}
$$

Equations (1) and (2) contain the static-equilibrium equations for the first and second phases of climbing obtained from the postures of the robot shown in Figs. 4(a)-(b). In the first phase, only link 1 is climbing while the other links(and wheels) are on the ground supplying the required push force, as shown in Fig. 4(a). Similarly, in the second phase, links 1 and 2 are involved in climbing at any instant, as shown in Fig. 4 (b). It is expected that the robot can climb heights upto $lsin\theta_{to}$ with just one climbing link and would need two climbing links for heights between $lsin\theta_{to}$ and $2lsin\theta_{to}$. In this paper, the analysis is limited to heights requiring at most 2 climbing links, thus ensuring that there are always

2 wheel-pairs on the ground to provide sufficient traction at any given point.

It can be seen that there are 5 equations per phase. The first 2 equations ensure the equilibrium of forces in the $x$ and $y$ directions, respectively. The remaining equations denote the moment equilibrium at the 2 link joints $J_1$ and $J_2$, and a wheel joint $R_3$, respectively. Note that, $w_w = 2m_w g$ and $w_l = m_l g$ where $m_w$ and $m_l$ denote the masses of the wheel and link, respectively. $F_i$ and $N_i$ are the traction and normal forces acting on $i^{th}$ wheel, respectively. $k_i$ is the spring constant of the spring acting at the $i^{th}$ link joint to maintain static equilibrium at an arbitrary configuration.

### C. Compliant Modular Robot

In the earlier section, it is explained that a generic set of static stability equations cannot be employed for analyzing and optimizing the modular robot's step climbing maneuver as it was shown in [11]. In the PAW([11]) robot and other passive suspension robots like SHRIMP([2]) and CRAB([4]), wheels always maintained contact with the ground. But in the case of the proposed robot, wheel-pairs may lift off the ground, where necessary, to avoid tip over. This slightly complicates the quasi static analysis as the static equilibrium equations change when there is a phase change during the climbing maneuver. The novelty of this work is in using compliant elements like springs to passively ensure that the robot doesn't tip over and thus develop a more energy efficient climbing maneuver.

One may note from equations in (1) that the maximum moment(due to normal and traction forces) is generated at link joint $J_1$ in the first phase, when only one link is climbing. Ideally, the spring should be stiff enough to resist this moment and eventually lift the second wheel-pair off the ground before $\phi_1$ reaches $\theta_{to}$. Once the second wheel is lifted off the ground, $\phi_1$ gradually decreases and $\phi_2$ starts increasing. This would constitute the phase-2 of the climb which is governed by the equations in (2). Eventually, $\phi_2$ also reaches the tip over angle, if the step is high enough. It is desired that the spring at link joint $J_2$ is stiff enough to resist and lift wheel 3 off the ground before that.

Using the fourth equation in (1), one can estimate the moment required to make $N_2 = 0$. It is assumed that all the wheels are rotating such that $\tau_w = min(\mu N_i, \tau_{wmax})$, where $\mu$ is 1, and $N_3$ and $N_4$ are equal to $N_{avg} = (4w_w + 3w_l)/4$. $\mu$ is assumed to be 1 as it is desired that the springs used are able to restrict the maximum moment that can be generated by the traction of all the wheels. Though this analysis starts with the assumption that $mu = 1$, eventually, the aim is to find the least value of the friction coefficient, $mu$, for which the robot is statically stable throughout the climbing phase. As $\phi_2 = 0$, the spring at joint $J_2$ will not apply any counter moment. Substituting the same, the moment required to lift the wheel off the ground can be obtained. The slope of the moment with the maximum joint angle $\theta_{to}$ gives, the desired stiffness. This implies that, when the first link reaches the tip over angle, enough counter moment is generated by the spring at the joint $J_1$ to lift wheel 2 off the ground. In this case, the stiffness of spring 1, $k_1$ is obtained as $2.82\ Nm/rad$. Similarly, the spring stiffness at joint $J_2$ is determined by first calculating the moment required to lift wheel 3 off the ground in the same fashion. The final equation in (2) is used for this analysis. Here, only $N_4 = N_{avg}$ while all other assumptions remain the same. Therefore, the spring constant $k_2$ for spring 2 is obtained as $8.10\ Nm/rad$. In this way, compliant joints are designed to avoid tip over and thus aid in reducing the energy expended to maintain stability during traversal. Springs also help in redistributing the normal forces among the remaining climbing wheel-pairs, when a wheel-pair is lifted off the ground.

With the addition of springs at the link joints, this modular robot can successfully climb steps upto twice its link length with the help of only wheel traction. However, wheel torques can control this step climbing only under the assumption that there will be no slippage. So this passive robot design cannot be fully exploited without ensuring that wheel slip is minimized. In the next section, the causes of wheel slip are discussed and an optimization routine with an objective to avoid slippage is described.

## III. Wheel Slip Reduction

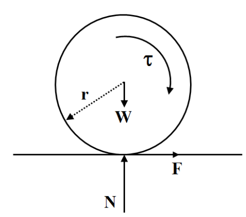


Fig. 5: Free body diagram of the wheel

Figure 5 shows the free-body diagram of a wheel rolling on a flat surface. It can be noted that, the wheel is in static equilibrium when $F = \tau/r$, where $r$ and $\tau$ are the wheel‘s radius and torque, respectively. For the wheel to maintain pure rolling, the frictional force $F$ should always satisfy the friction constraint equations, $F = \mu_s N$, where $\mu_s$ is the coefficient of static friction. Here, $F$ is directly proportional to the wheel torque $\tau$. If the wheel torque exceeds $\mu_s N$, then the wheel begins to slip and frictional force, $F = \mu_d N$, where $\mu_d$ is the coefficient of dynamic friction. The aim is to always keep the wheel torque within the limit of $\mu_s N$ to avoid any slippage. However, this is very hard to achieve as the the $\mu$ coefficient of the wheel-ground interface is not known beforehand and it also changes dynamically on any terrain. Well known slip reduction technologies like Anti-Lock Braking System (ABS), which is used extensively in automobiles, are equipped with sensors to detect wheel slip and then a corrective torque control action is taken till the wheel stops slipping. But this method requires slip to occur. A preventive method, which is not only robust but also exploits the robot's suspension mechanism to minimize slippage is desirable. Note that, for this analysis, it is assumed that the wheels rotate with a constant velocity.

To develop the analysis, one may first begin by assuming that there is no slip, and then estimate the $F_i$ and $N_i$ values across various points on the terrain by minimizing $\sum_i F_i/N_i$ to achieve this objective of no slip. For each wheel, this procedure estimates the least wheel-ground friction coefficient value for which the proposed robot doesn't slip. Denote the maximum value of the $F_i/N_i$ ratio obtained from this optimization as $\mu_o$. The mechanism with lower $\mu_o$ can traverse on a wider spectrum of surfaces without slipping.

Note that, slippage doesn't hinder the climbing ability of this robot. The robot can still successfully climb even if there is slip in some of its wheels. However, slip makes it difficult to exercise control on the robot and also wastes power. Therefore, it is very important to study it carefully and create mechanisms which can minimize slip.

### A. Posture Estimation

It is important to estimate posture of the robot at various heights during the climbing phase. The use of 2-links for climbing at any instant, allows the robot to climb steps/walls as high as $2lsin(\theta_{to})$(i.e., $h_{max}$) without tipping over as explained in Section-III. To estimate the postures, the step height is divided into $n$ set points between 0 and $h_{max}$, each point separated by a distance of $0.01m$. The posture of the robot at all the set points is determined so that they can to used to derive the static stability equations for that posture. For step heights that involve only one climbing link i.e., heights between 0 and $lsin(\theta_{to})$ (phase-1), the posture of the robot, in terms of the joint angles, can be determined as $\phi_1^j = sin^{-1}(h^j/l)$ and $\phi_2 = 0$. When $\phi_1 = 70^0$ $(phi_1 \approx \theta_{to})$ , i.e., after having climbed a height of 0.14m, the robot transitions to phase-2. Wheel-pair-2 is lifted off the ground and the robot now has two climbing members. This process reduces $\phi_1$ and increases $\phi_2$ while ensuring that $\theta_1 \leq \theta_{to}$. The desired postures for the second phase can be obtained by running a simple optimization procedure for all the heights between $lsin_{to}$ and $2lsin_{to}$ as shown in (3). The objective function ensures the net change in the relative angles is minimized while moving from one set-point to the other. This is very important from the quasi-static point of view as a drastic change in posture with a small increase in height cannot be attained without taking the dynamics of the system into consideration.

$$\begin{aligned} \underset{\phi_1,\phi_2}{\text{minimize}} \quad & \sum_{i=1}^{2}(\phi_i^j - \phi_i^{j-1})^2 \\ \text{subject to} \quad & lsin(\phi_1+\phi_2) + lsin(\phi_2) = h^j \\ & \phi_1 + \phi_2 \leq \theta_{to} \\ & 0 \leq \phi_1, \phi_2 \leq \theta_{to} \end{aligned} \tag{3}$$

This provides the posture desired from the robot at various set-points. The $F/N$ ratio has to be minimized across all these set-points to estimate the robot's performance and localize potential regions for slippage.

### B. Optimization Routine

Wheel torque optimization is a very active research area and several instances of successful application of wheel torque control for mobile robots, like SHRIMP [2] and CRAB [10], have been reported earlier in [7], [8], [5], [4]. A detailed study of this method is given in [6]. As explained in the earlier sections, all these robots have wheels maintaining ground contact during traversal. The proposed optimization is based on the quasi-static model of the robot, and is performed in the phased manner. Depending of the set point height, a different set of static stability equations are used as constraints for the optimization routine.

The objective of this optimization procedure is to estimate the least $F_i/N_i$ values for all the wheel-pairs at all the set points between 0 and $h_{max}$. Two optimization procedures are carried out for the two climbing phases. The objective function will remain the same for both the procedures, and is given in (4).

$$\sum_{i=1}^{4} F_i/N_i \tag{4}$$

The design variables are $F_i$'s and $N_i$'s of all the four wheels. For maintaining an arbitrary posture of the robot, the static equilibrium equations have to be satisfied at that posture. Thus, they form the equality constraints to this problem. These equations change from one phase to the other at the set point $lsin\theta_{to}$, to reflect the fact that the second wheel is lifted off the ground. Therefore, for phase-1, the equality constraints are obtained from (1) and for phase-2, it is obtained from (2). As the posture is predetermined for a given height, the equality constraints are linear. However, since the objective function is non-linear, Simplex method cannot be used to search for an optimal solution along the vertices of the convex polygon that denotes the feasible region. The entire feasible region has to be explicitly searched to obtain a global optimal solution. This is computationally intensive and standard functions like $fmincon$ (of MATLAB) rely on a strong initial guess provided by the user, to narrow down their search. Providing a good initial guess is hard in this scenario as the optimization routine has to be run on all the set points and each one may have a good initial guess of its own. An alternative approach is to further compress the feasible region by tightly bounding the design variables using the knowledge of their properties and the desired objective. To this end, additional linear inequality constraints are added to the system to reduce the feasible region and ensure that the proximity of the obtained solution is as close to the global minimum as possible. Equation (5) is to restrict the optimal $F/N$ ratio to always remain between 0 and 1 for all the wheels and at all the set points. Equation (6) bounds the wheel motor torques for all the wheels with

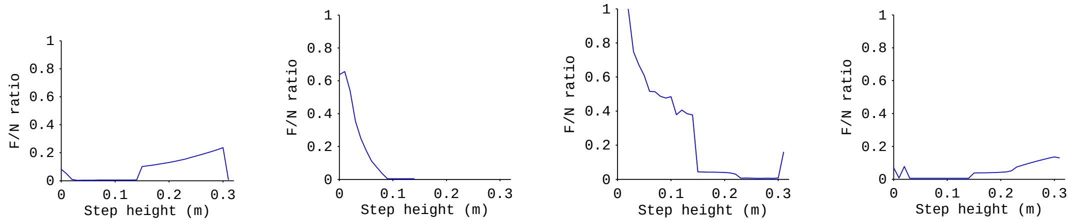


(a) Wheel 1 (b) Wheel 2 (c) Wheel 3 (d) Wheel 4

Fig. 6: Optimized $F/N$ values for all the wheels

their maximum values. Finally, the ratio will also decrease if normal $N$ increases. Therefore, equations in (7) ensures that the search space consists of only regions where $N$ increases or maintains atleast $N_{avg}$, viz. the normal force on a flat terrain. Additionally, for phase 2, $F_2$ and $N_2$ are equated to 0 as wheel 2 is lifted off the ground and its traction no longer contributes to step climbing.

$$F_i \leq N_i \quad \forall\ i = 1 \ldots 4 \tag{5}$$

$$0 \leq F_i \leq \tau_{wmax}/r \quad \forall\ i = 1 \ldots 4 \tag{6}$$

$$\begin{aligned} phase\ 1: \quad N_i \geq N_{avg} \qquad & i \in \{2,3,4\} \\ phase\ 2: \quad N_i \geq N_{avg} \qquad & i \in \{3,4\} \end{aligned} \tag{7}$$

The above mentioned optimization routine is performed for step of height 0.310m and at all its intermediate set points. The results are presented and discussed in the next section.

## IV. Results and Simulation

The optimal $F/N$ ratios for all the wheels thus obtained are plotted against the various height set-points, as shown in Figure 6. It can be noted from Figure 6(a) that, for wheel-pair-1, the $F/N$ ratio is consistently lower (max $F_1/N_1$ = 0.2357) as compared to all other wheels and especially lower in phase 1. In phase-1, all the three wheel torques combine to provide the horizontal normal force $N_1$. Thus, $N_1$ is always greater than or equal to $3N_{avg}$. Even though the required wheel torque for rolling might remain the same while climbing the step, the normal force has more than tripled thus greatly reducing $F_1/N_1$. This implies that this robot can climb on a very slippery surface without slipping as the reduction in $\mu_s$ is being compensated by increase in normal force $N$. This is the key novelty of modularity that this robot design wishes to exploit. For phase-2 however, the normal force $N_1 \geq 2N_{avg}$. Therefore, this robot can climb a step without slipping even if $\mu_s$ drops to a third of its original value in phase-1 or to half its value in phase-2. This makes this robot mechanism robust to changes in $\mu_s$ during step climbing.

For wheel-pair-2, as shown in Figure 6(b), $F_2/N_2$ reduces with an increase in height as $N_2$ increases in this process. However, in phase-2, wheel-pair-2 is not actuated as it can no longer provide traction. For wheel-pair-3, as shown in Figure 6(c), a trend similar to that of wheel-pair-2 is observed. It starts decreasing appreciably in phase-2 when wheel-pair-2 is off the ground as $N_3$ increases. Wheel-pair-4 has a counter intuitive trend. The average $F_4/N_4$ value is 0.0483 which is very low. However, the ratio increases in phase 2 instead of decreasing as in the case of other wheels. When the second wheel-pair is lifted off the ground, to maintain static equilibrium in the x-direction, forces are redistributed thus increasing the values of $F_3$ and $F_4$. However, for wheel-pair-3, $N_3$ also increases accordingly and therefore the ratio could be kept lower. The normal force $N_4$, on the other hand, doesn't increase proportionally thus increasing the ration in the case of wheel-pair-4.

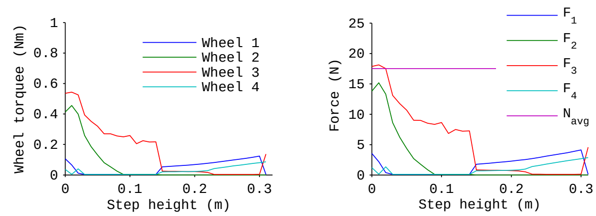


(a) Wheel torques (b) Frictional forces

Fig. 7: Plots of optimized wheel torques and frictional forces against step height for all the 4 wheels

From the quasi-static analysis, one can conclude that wheel-pair-3 is most susceptible to slip while step climbing followed by wheel 2. The design ensures that any wheel that is climbing the step is always least susceptible to slip. However, this analysis only provides wheel torque requirements to maintain a desired posture of the robot at a certain step height. But in a practical scenario, the robot will have to move from one set point to the other to make its way from the bottom of the step to the top. Generally, robots moving on a rough terrain move slowly with a constant velocity as discussed in [7]. To achieve the desired constant velocity, additional wheel torque needs to be supplied. The implications of combining velocity control model with this optimized wheel torque model is discussed in the next subsection.

Figure 7(a) shows the wheel torques required to maintain static stability at various heights between $0$ and $h_{max}$. The saturation torque of all the wheel motors is $1Nm$. However, the maximum torque that was generated during this routine was only $0.53Nm$, by wheel-pair-3. So the torque requirements are well within the range. Figure 7(b) shows the same curves from the frictional force perspective and compares them to the average normal force $N_{avg}$. This makes it clear that wheel-pair-3 will slip even if $\mu = 1$, for step heights less than $0.03$m and its slippage will only worsen with the addition of velocity control or when $\mu$ is low. Wheel-pair-2 is the next most susceptible to slip on surfaces with low $\mu_s$ values. It can be noted that wheel-pairs-1 and -4 require very little torque to attain static equilibrium and they can apply much greater torque without causing slippage. Therefore, to reduce slip the robot should be made to travel on the step with a higher velocity that on the flat ground. This way, the climbing members will reach phase-2 sooner thus ensuring that wheels 2 and 3 don't slip long enough. This can be achieved without much slip at wheel-pair-1 due to the high $N_1$ value. These insights, if incorporated into an wheel velocity controller, can lead to an efficient climbing manoeuvre which is energy efficient and robust to the frictional properties of the surface.

## V. Conclusions and Future Work

This paper proposes a wheel-torque optimization of a modular wheeled robot with compliant link-joints. A detailed quasi-static analysis of the model is presented, and used to determine optimal spring stiffness values for each link-joint. It has been shown that the robot is able to negotiate steps whose heights are upto twice its module's link length using only wheel traction. Next, wheel torque optimization is presented to minimize wheel-slip leading to better control and energy efficient climbing. This also helps in predicting wheel-slip of the robot on wheel-ground contacts with known coefficients of friction. The proposed approach lends utility in determining the maximum velocity that the robot can attain without slipping, and designing a wheel torque controller for step climbing.

Implementation of the proposed framework for the control of an actual prototype will be carried out in future. A similar wheel torque optimization for climbing down motion will also be investigated. The present study ignores rolling resistance which will be incorporated in the future work.

## References

[1] Richard Volpe, J. Balaram, Timothy Ohm, Robert Ivlev, and Prototype Rocky. Rocky 7: A next generation mars rover prototype. *Journal of Advanced Robotics*, 11:341–358, 1997.

[2] T. Estier, Y. Crausaz, B. Merminod, M. Lauria, R. Piguet, and R. Siegwart. An innovative space rover with extended climbing abilities. *Proceedings of Space and Robotics*, 2000:333–339, 2000.

[3] C. Grand, F. BenAmar, F. Plumet, and P. Bidaud. Decoupled control of posture and trajectory of the hybrid wheel-legged robot hylos. In *IEEE International Conference on Robotics and Automation(ICRA), New Orleans, USA*, 2004.

[4] K. Turker, I. Sharf, and M. Trentini. Step negotiation with wheel traction: a strategy for a wheel-legged robot. In *IEEE International Conference on Robotics and Automation (ICRA), St. Paul, USA*, 2012.

[5] Mark Yim, Wei-Min Shen, Behnam Salemi, Daniela Rus, Mark Moll, Hod Lipson, Eric Klavins, and Gregory S Chirikjian. Modular self-reconfigurable robot systems [grand challenges of robotics]. *IEEE Robotics & Automation Magazine*, 14(1):43–52, 2007.

[6] S Avinash, V V Anurag, A K Singh, S V Shah, and K M Krishna. A semi-active robot for steep obstacle ascent. In *IEEE Multi-Conference on Systems and Control (MSC), Hyderabad, India*, 2013.

[7] A.K. Singh, R.K. Namdev, V. Eathakota, and K.M. Krishna. A novel compliant rover for rough terrain mobility. In *IEEE/RSJ International Conference on Intelligent Robots and Systems (IROS), Taipei, Taiwan*, 2010.

[8] Ambroise Krebs, Fabian Risch, Thomas Thueer, Jérôme Maye, Cédric Pradalier, and Roland Siegwart. Rover control based on an optimal torque distribution-application to 6 motorized wheels passive rover. In *IEEE/RSJ International Conference on Intelligent Robots and Systems (IROS), Taipei, Taiwan*, 2010.

[9] Thomas Thueer, Pierre Lamon, Ambroise Krebs, and Roland Siegwart. Crab-exploration rover with advanced obstacle negotiation capabilities. In *Proceedings of the 9th ESA Workshop on Advanced Space Technologies for Robotics and Automation (ASTRA), Noordwijk, The Netherlands*, 2006.

[10] Pierre Lamon, Ambroise Krebs, Michel Lauria, Roland Siegwart, and Steven Shooter. Wheel torque control for a rough terrain rover. In *IEEE International Conference on Robotics and Automation (ICRA), New Orleans, USA*, 2004.

[11] P. Lamon and R. Siegwart. Wheel torque control in rough terrain-modeling and simulation. In *IEEE International Conference on Robotics and Automation (ICRA), Barcelona, Spain*, 2005.

[12] Ambroise Krebs, Thomas Thueer, Edgar Carrasco, and Roland Siegwart. Towards torque control of the crab rover. In *Proceedings of the 9 th International Symposium on Artificial Intelligence, Robotics and Automation in Space (iSAIRAS), Los Angeles, USA*, 2008.

[13] Ambroise Krebs, Thomas Thueer, Stéphane Michaud, and Roland Siegwart. Performance optimization of all-terrain robots: a 2d quasi-static tool. In *IEEE/RSJ International Conference on Intelligent Robots and Systems (IROS), Beijing, China*, 2006.